

## The Permeability of the Frog Choroid Plexus to Nonelectrolytes

ERNEST M. WRIGHT and JOHN W. PRATHER \*

Department of Physiology, University of California Medical Center,  
Los Angeles, California 90024

Received 18 November 1969

*Summary.* An *in vitro* preparation of the frog choroid plexus has been used to measure the permeability of the choroidal epithelium to 50 nonelectrolytes by an osmotic method. The method involves the measurement of nonelectrolyte reflection coefficients ( $\sigma$ ) by a rapid electrical procedure. For the majority of compounds tested, there was a good correlation between the rate of solute permeation and the solute's bulk-phase lipid:water partition coefficients; i.e., the higher the partition coefficient the greater the permeability. The membrane lipids of the choroid plexus differ from the membrane lipids of the gall bladder in at least three ways: (1) the lipids of the choroid plexus cannot distinguish between branched chain solutes and their straight chain isomers; (2) small polar solutes such as urea and acetamide permeate via the membrane lipids to a significant extent; and (3) the smaller selectivity ratios suggest that the lipids of the choroid plexus contain more hydrogen bonding sites (i.e., there are stronger solute:lipid intermolecular forces in the choroid plexus). The permeability characteristics of the choroid plexus are qualitatively similar to those of most other cell membranes. In addition, there is evidence for the presence of a special mechanism for the transport of sugar across this epithelium.

It is generally accepted that the choroid plexuses are the major source of the cerebrospinal fluid (CSF). This fluid buffers the neurones of the central nervous system against wide fluctuations in the composition of plasma; e.g., ions which critically affect the function of the nervous system, such as  $K^+$ ,  $Ca^{++}$  and  $Mg^{++}$ , are maintained at constant concentrations in the CSF. The mechanisms by which the choroidal epithelium elaborates the CSF are not yet well understood (*see* review by Davson, 1967). The development of an *in vitro* preparation of the frog posterior choroid plexus has enabled us to elucidate certain properties of the choroidal epithelium. The present paper describes this preparation and discusses the mechanism of nonelectrolyte permeation through the epithelium; the accompanying

---

\* Present address: AMES-Bioengineering Department, University of California, La Jolla, California 92037.

paper (Prather & Wright, 1970) describes the mode of sugar transport in detail. Subsequent papers will pertain to ion transport across the isolated choroid plexus.

The permeability of the plexus to nonelectrolytes was determined by the method first introduced for the small intestine by Smyth and Wright (1966) and later used by Wright and Diamond (Wright & Diamond, 1969*a, b*; Diamond & Wright, 1969*a*) in their investigation of nonelectrolyte permeation in the gallbladder epithelium. This study provides a background to the physiology of the choroid plexus and, in addition, yields data for a comparison of nonelectrolyte permeation mechanisms in the gallbladder and choroid plexus.

### Materials and Methods

In this project we have used the choroid plexus from the IVth ventricle of the bullfrog *Rana catesbeiana*. In lower vertebrates such as amphibians and elasmobranch fishes, this plexus, sometimes known as the posterior choroid plexus, forms the roof of the open IVth ventricle. The ventricular surface of the membrane is highly folded due to villus-like projections which extend about 1.5 mm into the ventricle. The villi are covered with a cuboidal epithelium and contain a network of blood vessels surrounded by a loose connective tissue. The structure of the frog posterior choroid plexus closely resembles that in the *Necturus* which has already been described in some detail by Carpenter (1966).

The choroid plexus was removed from the excised brain by carefully cutting along the lateral and anterior edges of the highly pigmented membrane. The plexus was then mounted between two lucite half-chambers which were similar in design to those described by Lasansky and de Fisch (1966). The area of the window between the chambers was 2.6 mm<sup>2</sup>, and the volume of the saline in each half-chamber was 1.5 ml. These saline solutions were stirred by streams of water-saturated oxygen bubbles injected through syringe needles; the saline could be replaced by the use of syringes. The saline in contact with the brush border of the epithelium is referred to as the ventricular solution, whereas that in contact with the vascular side of the epithelium is referred to as the serosal solution.

### Electrical Measurements

The electrical potential difference (p. d.) across the choroid plexus was recorded by connecting the ventricular and serosal solutions to a Keithley electrometer, model 610 B, by means of salt bridges and calomel half-cells. The output of the electrometer was displayed on a Varian potentiometric chart recorder, model G11A, and the p. d. were measured to within 0.01 mV. All p. d.'s were corrected for the asymmetry of the electrical circuit which was generally less than 0.25 mV. The salt bridges consisted of polyethylene tubing filled with 110 mM NaCl in 4% agar; each was placed 1 mm from the surface of the membrane.

The conductance of the membrane was measured by observing the potential drop when a direct current was passed across the tissue. The potential assumed a new steady value within the response time of the recorder (ca. 1 sec), and no transients were noted. The current, tapped off potentiometrically from a battery, was measured on a Keithley

600 A electrometer and passed to the opposite sides of the plexus via Ag/AgCl electrodes and salt bridges. The conductances were corrected for the conductance of the saline between the tips of the salt bridges used to monitor the p.d.

### *Solutions*

The Ringer's solution used in these experiments contained 110 mM NaCl, 2 mM KCl and 1.0 mM CaCl<sub>2</sub>, buffered at pH 8.2 with 0.4 mM imidazole. In a few experiments, mentioned specifically in the text, the pH of the saline was varied between 2.6 and 10.7, the calcium concentration was varied between 0.25 and 5 mM, and the high calcium concentration was replaced with 5 mM MgCl<sub>2</sub>, BaCl<sub>2</sub> or SrCl<sub>2</sub>. The following buffers were used when the pH of the saline was varied: 1.6 mM glycine and NaOH, pH 9.7 to 10.7; 2.5 mM Na<sub>2</sub>HPO<sub>4</sub>-NaH<sub>2</sub>PO<sub>4</sub>, pH 5.4 to 7.1; 1.6 mM potassium phthalate and NaOH or HCl, pH 2.6 to 4.4. The pH of the solutions was measured with a glass electrode. In the solutions containing high concentrations of the alkaline earth cations, no attempt was made to compensate for the slight variations in osmolarity.

Nonelectrolytes were added to the Ringer's solutions to give a concentration of 100 mmolal, and all compounds were of the highest purity commercially available, generally from either Eastman Organic Chemicals (Rochester, N.Y.) or Aldrich Chemical Co., Inc. (Milwaukee, Wisc.). In addition, on the basis of previous experience (Wright & Diamond, 1969*a, b*), we used only those compounds which were known to be stable, and not to produce changes in pH or anomalous osmolarities. The osmolarity of nonelectrolyte solutions was checked with a Fiske osmometer.

### *Animals*

All bullfrogs used in this study were obtained from local suppliers and were maintained at room temperature for about 2 weeks prior to use. Experiments were carried out at room temperature which ranged from 22 to 24 °C.

The variance is indicated by standard deviations.

## **Results**

### *Electrical Potentials and Conductance*

The p.d. recorded across the *in vitro* choroid plexus was usually less than 1 mV. The value of this potential in 29 experiments was  $0.32 \pm 0.48$  mV, the ventricular solution being positive with respect to the serosal solution. Within the first few minutes of mounting the choroid plexus in the chamber, the p.d. usually decayed a fraction of a millivolt but thereafter remained constant for at least 6 hr. Neither the addition of glucose (5 to 10 mM) to the saline nor anoxia produced any significant change in the p.d. The conductance of the choroid plexus 3 hr after the preparation was set up was  $13.7 \pm 2.8(6)$  mmhos  $\times$  cm<sup>-2</sup>. In two experiments, the conductance increased by about 6% per hour. These observations are very similar to those reported for the isolated choroid plexus of the dogfish (Patlak, Adamson, Oppelt & Rall, 1966).

### *Streaming Potentials*

The osmotic flow of water across charged membranes generates electrical potentials which may be called streaming potentials.<sup>1</sup> These potentials have been observed in the gallbladder (Diamond, 1962; Pidot & Diamond, 1964; Dietschy, 1964), in the small intestine (Smyth & Wright, 1966), and in nerve (Vargas, 1968). The effect of osmotic gradients on the p.d. across the choroid plexus has been tested, and an experiment illustrating the results is shown in Fig. 1. When the ventricular solution was replaced with a solution identical in ionic composition but containing in addition 100 mmolal sucrose, the ventricular solution became positive by 1.35 mV. This p.d. built up with a half time of 65 sec: on restoring the sucrose-free saline to the ventricular side of the membrane, the p.d. decayed to the original level with approximately the same time constant. In 14 choroid plexuses, the average value of the streaming potential was  $1.9 \pm 0.63$  mV/100 mmolal sucrose, and the average half time for the build up was  $68 \pm 14$  sec.

The slow buildup of the streaming potential probably reflects the time required for sucrose to reach its final concentration in the unstirred layer adjacent to the surface of the membrane. The half time for the change in concentration, and hence the half time ( $t_{1/2}$ ) for the potential change, is inversely proportional to the sucrose diffusion coefficient ( $D$ ) and directly proportional to the thickness of the unstirred layer ( $\delta$ ); i.e.,  $t_{1/2} = 0.38 \delta^2/D$  (Diamond, 1966). The thickness of the unstirred layer on the ventricular side of the choroid plexus is therefore about 300  $\mu$ . The highly folded surface of the membrane would account for this rather thick unstirred layer.

In three experiments, we compared the effect of sucrose in the serosal solution with the effect of sucrose in the ventricular solution. When the serosal solution was made hypertonic with sucrose (100 mmolal), the magnitude of the streaming potential was, on the average, 55% less than the streaming potential generated from the ventricular solution, and the  $t_{1/2}$  for the change in potential increased to about 230 sec. These quantitative differences between the streaming potentials are probably related to the structure of the tissue. For example, the presence of connective tissue between the epithelium and the serosal solution and/or the lateral spaces between the epithelial cells may increase the sweeping-away effects (*see*

<sup>1</sup> It has been suggested by Schmid and Schwarz (1952) that the electrical potentials associated with osmotic flow across membranes have three components: the true electrokinetic streaming potential; a boundary diffusion potential, which is associated with the unstirred layers adjacent to the membrane; and a profile asymmetry potential, owing to the fact that water flow across the membrane may perturb the ion concentration profile within the membrane. In the present paper, the term "streaming potential" is used to refer to the total potential associated with osmotic flow. *See also Discussion.*

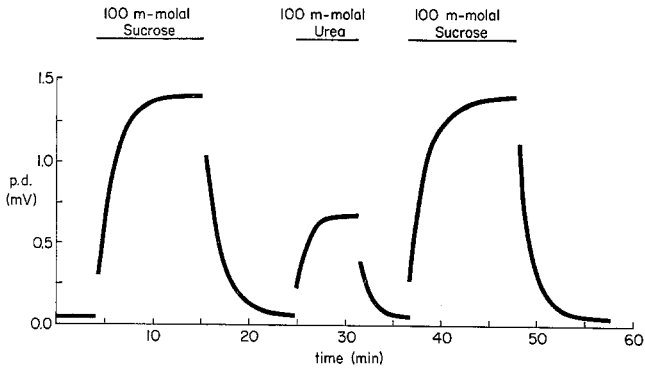


Fig. 1. The experimental procedure for determining nonelectrolyte reflection coefficients in the frog choroid plexus. The ordinate shows the electrical potential across the tissue, ventricular solution positive with respect to the serosal solution; the abscissa shows time. The ventricular solution was replaced with Ringer's solution containing either 100 mmolal sucrose or 100 mmolal urea at the times indicated. The serosal solution was Ringer's throughout the experiment

next section) in the unstirred layer immediately adjacent to the serosal face of the epithelium. A larger sweeping-away effect, due to an increase in the linear velocity of water flow and a decrease in the apparent diffusion coefficients in the connective tissue and/or lateral spaces, would reduce the effective serosal sucrose concentration and produce a smaller osmotic flow and a lower streaming potential. The reduction in the apparent sucrose diffusion coefficient would also explain the increase in  $t_{1/2}$ , as it is unlikely that the thickness of the unstirred layer on the serosal side of the tissue is much greater than that on the ventricular side.

The effect of varying the sucrose concentration in the ventricular solution is shown in Fig. 2. The magnitude of the induced potential was a linear function of the sucrose concentration up to 100 mmolal. This was confirmed in four other experiments where, in addition, we observed that the proportionality constant between streaming potential and sucrose concentration decreased at concentrations of 200 to 300 mmolal.

The effect of pH on the streaming potential was determined by varying the pH of both the ventricular and serosal solutions from 2.4 to 10.7, and recording the magnitude of the potential caused by 100 mmolal sucrose in the ventricular solution. The p.d. in the absence of osmotic gradients was relatively insensitive to pH. A streaming potential was first recorded at pH 8.2, then after changing the pH of the solutions to some new value, and finally when the pH was returned to 8.2. There was little or no effect on the streaming potential over the range 6.1 to 10.7, but below pH 6.1 the

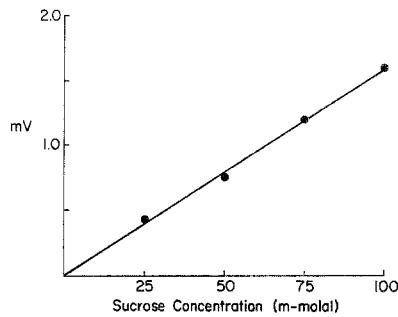


Fig. 2. The relation between streaming potential and sucrose concentration. The ordinate shows the streaming potential across the choroid plexus; the abscissa shows the sucrose concentration in the ventricular solution

p.d. decreased with increasing hydrogen ion concentrations. At the lowest pH tested, pH 2.6, there was an actual reversal in the polarity of the streaming potential; i.e., the ventricular solution became negative. In the three choroid plexuses where the entire range of pH values was tested, the isoelectric point and apparent  $pK_a$  were pH 3 and pH 4, respectively. These results are very similar to those reported and discussed previously for the effect of pH on streaming potentials in the small intestine (Smyth & Wright, 1966) and gallbladder (Wright & Diamond, 1968).

In the rabbit gallbladder, streaming potentials are a function of the calcium concentration in the external bathing solutions (Diamond & Harrison, 1966; Wright & Diamond, 1968). We have investigated the effect of calcium on the choroid plexus by measuring streaming potentials at low and high calcium concentrations. In these experiments, streaming potentials were measured in Ringer's solution containing 0.25 mM  $\text{CaCl}_2$ , in solutions where the calcium concentration was raised to 5 mM in both the ventricular and serosal solutions, and finally in solutions when the calcium concentration was returned to the lower level. In four experiments, increasing the calcium concentration produced no significant effect on the streaming potential. However, in these four experiments, we also compared the effects of Ca, Sr, Ba and Mg by replacing the  $\text{CaCl}_2$  in both the ventricular and serosal solutions with 5 mM Ba-, Sr- or  $\text{MgCl}$ . Barium reduced the streaming potential by  $30 \pm 7\%$  in the four experiments, but neither magnesium nor strontium produced any significant effect. Although there are 24 possible permutations of the 4 alkaline earth cations, only 7 of these are commonly observed in biological systems. These seven selectivity sequences are predictable from Coulomb forces and the free energy of hydration of the

cations.<sup>2</sup> The choroid plexus sequence (Ba > Ca, Sr, Mg) is either sequence I or II (see Fig. 2 of Diamond & Wright, 1969b).

Streaming potentials produced by osmotic gradients across the choroid plexus are therefore qualitatively very similar to those observed in the gallbladder, small intestine and nerve.

### *Determination of Reflection Coefficients*

The parameter used to measure the permeability of the choroid plexus to nonelectrolytes was the reflection coefficient.

Reflection coefficients, or Staverman coefficients, are defined as the ratio of the osmotic flow produced by a concentration gradient of the test solute to the flow caused by the same concentration gradient of an impermeable solute (Staverman, 1948). The value of the reflection coefficient ( $\sigma$ ) depends on the nature of both the membrane and the test solute;  $\sigma$  for an impermeant solute is 1 (i.e., for an impermeant solute,  $\omega \bar{V}_s \ll L_p$ ), and for increasingly permeant solutes  $\sigma$  decreases progressively below 1. Negative values of  $\sigma$  are possible if the solute is more permeant than water. Reflection coefficients are related to permeability coefficients by an equation derived by Katchalsky and Kedem (1962),

$$\sigma = 1 - \frac{\omega \bar{V}_s}{L_p} - \frac{\omega f_{sm} d}{\phi_w} \quad (1)$$

where  $\omega$  is the solute permeability coefficient ( $\omega RT = P$ ),  $\bar{V}_s$  the partial molar volume of the solute,  $L_p$  the hydraulic conductivity of the membrane,  $f_{sm}$  the frictional coefficient between the solute and the membrane,  $d$  the membrane thickness, and  $\phi_w$  the volume fraction of water in the membrane. The first term  $\frac{\omega \bar{V}_s}{L_p}$ , represents the reduction in  $\sigma$  below 1 owing to the volume flow of solute across the membrane, and the second term,  $\frac{\omega f_{sm} d}{\phi_w}$ , represents the reduction due to frictional interaction between the solute and water in the membrane. This second term appears in the equation if, and only if, water and the solute interact while crossing the membrane. It is apparent from Eq. (1) that  $1 - \sigma$  increases with increasing permeability coefficients.

In addition to these thermodynamic effects,  $\sigma$ 's are reduced further by two unstirred-layer effects. (1) The flux of solute through the membrane tends to dissipate the concentration gradient across the membrane as a result of imperfect stirring close to the membrane. The concentration gradient is reduced by an amount  $\phi \frac{(\delta_1 + \delta_2)}{D}$ , where  $\phi$  is the flux of solute through the membrane,  $D$  the solute free-solution diffusion coefficient, and  $\delta_1$  and  $\delta_2$  the widths of the unstirred layers on each side of the membrane (Dainty, 1963). (2) The osmotic flow of water across a membrane also tends to reduce the effective concentration gradient by enhancing the solute concentration on the dilute side of the membrane and by depleting the solute concentration on the concentrated side of the membrane. The solute concentration adjacent to the membrane ( $C_m$ ) is

<sup>2</sup> Sherry (1969) predicted these seven sequences for closely spaced sites on the basis of the differences between the free energy of cation:site interactions and the free energy of cation hydration.

related to the bulk phase concentration ( $C_b$ ) by the expression

$$C_m = C_b \exp \pm \frac{V\delta}{D}, \quad (2)$$

where  $\delta$  is the thickness of the unstirred layer on that side of the membrane,  $D$  the free-solution diffusion coefficient of the particular solute, and  $V$  the velocity of water flow across the membrane (Dainty, 1963). The velocity of flow is negative for the sweeping-away effect on the concentrated side and positive for the enhancing effect at the dilute side.

Both of these types of unstirred-layer corrections apply to measurements of  $L_p$  and  $\omega$  as well as to  $\sigma$ . In the present study, the unstirred-layer corrections have been avoided by limiting the discussion to the kinds of conclusions that can be drawn without these corrections, e.g., the empirical relations between  $\sigma$  and other parameters such as partition coefficients.

Nonelectrolyte reflection coefficients were determined by making use of the fact that streaming potentials are directly proportional to the rate of osmotic flow. Owing to technical difficulties, this proportionality has yet to be confirmed in the choroid plexus; but in the gallbladder (Diamond, 1962, 1966; Pidot & Diamond, 1964), small intestine (Smyth & Wright, 1966) and nerve (Vargas, 1968), this fact is well established. In practice,  $\sigma$ 's were determined by measuring the streaming potentials produced by test solutes and by an impermeant solute. (See Wright & Diamond, 1969*a*, for a more detailed discussion of the principles involved.)

An actual experiment illustrating the procedure used to determine  $\sigma$  in the choroid plexus is shown in Fig. 1. As discussed earlier, the p.d. across the isolated choroid plexus is close to zero with identical Ringer's solutions in contact with each face of the tissue. A streaming potential of 1.35 mV was obtained when the ventricular solution was made hypertonic with 100 mmolal sucrose. A lower streaming potential, 0.63 mV, was obtained when the ventricular solution was made hypertonic with 100 mmolal urea. As expected from the higher urea diffusion coefficient, the half time for the buildup of the urea potential was about half that required for the buildup of the sucrose potential. Finally, sucrose gave a streaming potential of 1.35 mV, identical to the initial value, which showed that exposure of the choroid plexus to a high concentration of urea produced no adverse effect on the permeability properties of the tissue. Since the choroid plexus is virtually impermeable to sucrose (see Prather & Wright, 1970), and since streaming potentials are proportional to the rates of flow, the ratio of the streaming potentials (0.63:1.35) yields a urea reflection coefficient of 0.47. In 12 choroid plexuses, the average  $\sigma$  for urea was  $0.56 \pm 0.08$ .

Three groups of compounds were chosen in order to characterize non-electrolyte permeation through the choroid plexus: (1) relatively large



compounds (mol wt > 80) with ether:water partition coefficients ranging from  $5 \times 10^{-6}$  to  $9 \times 10^1$  were used to establish the relationship between permeation and partition coefficients; (2) small polar solutes (mol wt < 75, e.g., urea) were used to determine if small molecules permeate via polar regions in the membrane; and (3) branched-chain compounds and their isomers were used to probe the configuration of the membrane lipids. The Table summarizes the results. This table is arranged to facilitate comparison between the results obtained in the gallbladder (*see* Table 1 of Wright & Diamond, 1969*b*) and in the choroid plexus. For each of the 50 compounds listed, we have included the average value and standard deviation of  $\sigma$ , the chemical formula, the molecular weight and the ether:water partition coefficient.

### *Analysis of Results*

It is well established that the molecular forces which govern the rate of permeation of most nonelectrolytes through most biological membranes are the same as those that control the partition of these solutes between bulk lipid phases and water (Collander, 1954; Diamond & Wright, 1969*b*). Thus the permeability coefficient is given by the following expression:  $P = KD/d$ , where  $P = \omega RT$  is the permeability coefficient of the solute,  $D$  is the diffusion coefficient of that solute in the membrane lipid,  $K$  is the membrane lipid:water partition coefficient, and  $d$  is the thickness of the membrane. The nonelectrolyte  $\sigma$ 's in the Table have therefore been plotted as a function of their bulk phase partition coefficients. Since the partition coefficients for membrane lipid:water systems are unavailable, we have used ether:water partition coefficients; Collander (1947) has demonstrated that the partition coefficients in most lipid solvents correlate well with each other. Fig. 3 is a plot of  $\sigma$  against ether:water partition coefficients ( $K_{\text{ether}}$ ). At low values of  $K_{\text{ether}}$ ,  $\sigma$  is close to 1; as the partition coefficients increase,  $\sigma$ 's decrease towards 0, and eventually, at high values of  $K_{\text{ether}}$ , negative  $\sigma$ 's are obtained. Similar results were obtained when  $\sigma$ 's were plotted against olive oil:water and isobutanol:water partition coefficients. In other words, for the majority of the solutes tested, permeability increases with increasing lipid solubility.

The group of compounds numbered 1 to 5 in Fig. 3 are all low molecular weight compounds (mol wt < 75) with ether:water partition coefficients of less than 0.006. Note that the  $\sigma$ 's predicted for these five compounds from the main pattern are all below 1.0; i.e., despite their relatively low partition coefficients, they still permeate through the membrane lipid to a significant extent. For example, on the basis of the curve fitted to the higher

Table. *Choroid plexus reflection coefficients*

Compound <sup>a</sup>	Molecular formula	Mol Wt	Ether: water partition coefficient <sup>b</sup> ( $K_{\text{ether}}$ )	$\sigma^c$
<i>One-carbon compounds</i>				
Methanol	H <sub>3</sub> COH	32	0.14	-0.04 ± 0.03 (4)
Formamide	$\begin{array}{c} \text{O} \\    \\ \text{HC}-\text{NH}_2 \end{array}$	45	0.0014	0.08 ± 0.02 (6)
Urea	$\begin{array}{c} \text{O} \\    \\ \text{H}_2\text{N}-\text{C}-\text{NH}_2 \end{array}$	60	0.00047	0.56 ± 0.08 (12)
Thiourea	$\begin{array}{c} \text{S} \\    \\ \text{H}_2\text{N}-\text{C}-\text{NH}_2 \end{array}$	76	0.0063	0.50 ± 0.04 (5)
<i>Two-carbon compounds</i>				
Ethanol	H <sub>3</sub> C-CH <sub>2</sub> -OH	46	0.26	-0.03 ± 0.03 (4)
Ethylene glycol	HO-CH <sub>2</sub> -CH <sub>2</sub> -OH	62	0.0053	0.12 ± 0.05 (4)
Acetamide	$\begin{array}{c} \text{O} \\    \\ \text{H}_3\text{C}-\text{C}-\text{NH}_2 \end{array}$	59	0.0025	0.15 ± 0.05 (7)
Methyl urea	$\begin{array}{c} \text{O} \\    \\ \text{H}_3\text{C}-\text{NH}-\text{C}-\text{NH}_2 \end{array}$	74	0.0012	0.38 ± 0.07 (4)
Methyl thiourea	$\begin{array}{c} \text{S} \\    \\ \text{H}_3\text{C}-\text{NH}-\text{C}-\text{NH}_2 \end{array}$	90	—	0.26 ± 0.06 (4)
<i>Three-carbon compounds</i>				
n-Propanol	H <sub>3</sub> C-CH <sub>2</sub> -CH <sub>2</sub> -OH	60	1.9	-0.12 ± 0.03 (3)
Isopropanol	$\begin{array}{c} \text{CH}_3 \\   \\ \text{H}_3\text{C}-\text{CH}-\text{OH} \end{array}$	60	0.64	-0.03 ± 0.05 (4)
Methyl acetate	$\begin{array}{c} \text{O} \\    \\ \text{H}_3\text{C}-\text{C}-\text{OCH}_3 \end{array}$	74	2.7	-0.19 ± 0.05 (5)
1,3-Propanediol	HO-CH <sub>2</sub> -CH <sub>2</sub> -CH <sub>2</sub> -OH	76	0.012	0.17 ± 0.04 (5)
Glycerol	$\begin{array}{c} \text{OH} \quad \text{OH} \quad \text{OH} \\   \quad   \quad   \\ \text{CH}_2-\text{CH}-\text{CH}_2 \end{array}$	92	0.00066	0.81 ± 0.06 (5)

<sup>a</sup> Within each carbon grouping, compounds are arranged according to the number of nitrogen atoms, those with no nitrogen first. Within each subgrouping, compounds are arranged according to the number of oxygen atoms. Compounds in which oxygen was replaced with sulphur follow their oxygen analogues.

<sup>b</sup> Ether: water partition coefficients taken mostly from Collander, 1949.

<sup>c</sup> Average value, standard deviation, and total number of estimates of  $\sigma$ .

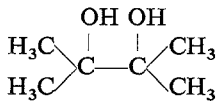
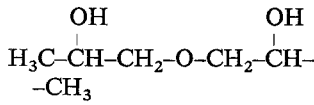
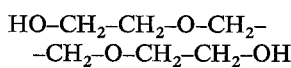
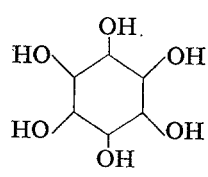
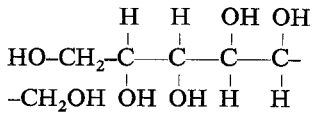
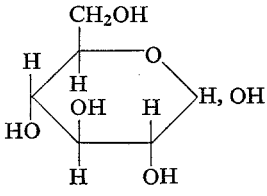
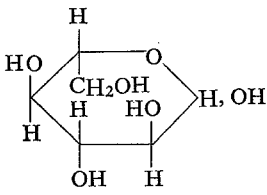
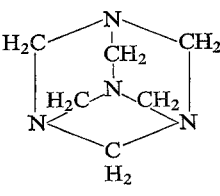
Table (continued)

Compound <sup>a</sup>	Molecular formula	Mol Wt	Ether: water partition coefficient ( $K_{\text{ether}}$ )	$\sigma^c$
Dihydroxy- acetone	$\begin{array}{c} \text{CH}_2-\text{C}-\text{CH}_2 \\   \quad    \quad   \\ \text{OH} \quad \text{O} \quad \text{OH} \end{array}$	90	—	$0.51 \pm 0.04(4)$
Propionamide	$\begin{array}{c} \text{O} \\    \\ \text{H}_3\text{C}-\text{CH}_2-\text{C}-\text{NH}_2 \end{array}$	73	0.013	$0.06 \pm 0.02(4)$
Ethyl urea	$\begin{array}{c} \text{O} \\    \\ \text{H}_3\text{C}-\text{CH}_2-\text{NH}-\text{C}-\text{NH}_2 \end{array}$	88	0.0041	$0.24 \pm 0.06(4)$
Ethyl thiourea	$\begin{array}{c} \text{S} \\    \\ \text{H}_3\text{C}-\text{CH}_2-\text{NH}-\text{C}-\text{NH}_2 \end{array}$	104	—	$0.11 \pm 0.01(4)$
Malonamide	$\begin{array}{c} \text{O} \quad \text{O} \\    \quad    \\ \text{H}_2\text{N}-\text{C}-\text{CH}_2-\text{C}-\text{NH}_2 \end{array}$	102	0.0003	$0.95 \pm 0.08(6)$
<i>Four-carbon compounds</i>				
n-Butanol	$\text{H}_3\text{C}-\text{CH}_2-\text{CH}_2-\text{CH}_2-\text{OH}$	74	7.7	$-0.22 \pm 0.10(4)$
sec-Butanol	$\begin{array}{c} \text{OH} \\   \\ \text{H}_3\text{C}-\text{CH}-\text{CH}_2-\text{CH}_3 \end{array}$	74	4.5	$-0.09 \pm 0.03(4)$
Ethyl acetate	$\begin{array}{c} \text{O} \\    \\ \text{H}_3\text{C}-\text{C}-\text{O}-\text{CH}_2-\text{CH}_3 \end{array}$	88	8.5	$-0.12 \pm 0.03(4)$
2,3-Butanediol	$\begin{array}{c} \text{OH} \quad \text{OH} \\   \quad   \\ \text{H}_3\text{C}-\text{CH}-\text{CH}-\text{CH}_3 \end{array}$	90	0.029	$0.05 \pm 0.06(5)$
1,4-Butanediol	$\begin{array}{c} \text{OH} \quad \quad \quad \text{OH} \\   \quad \quad \quad   \\ \text{H}_2\text{C}-\text{CH}_2-\text{CH}_2-\text{CH}_2 \end{array}$	90	0.019	$0.10 \pm 0.03(4)$
Ethylene glycol monoethyl ether	$\text{HO}-\text{CH}_2-\text{CH}_2-\text{O}-\text{CH}_2-\text{CH}_3$	90	0.20	$-0.06 \pm 0.04(4)$
Diethylene glycol	$\text{HO}-\text{CH}_2-\text{CH}_2-\text{O}-\text{CH}_2-\text{CH}_2-\text{O}-\text{CH}_2-\text{OH}$	106	0.004	$0.40 \pm 0.09(4)$
D-Erythritol	$\begin{array}{c} \text{H}_2\text{C}-\text{CH}-\text{CH}-\text{CH}_2 \\   \quad   \quad   \quad   \\ \text{HO} \quad \text{OH} \quad \text{OH} \quad \text{OH} \end{array}$	122	0.00011	$1.01 \pm 0.03(4)$
n-Butyramide	$\begin{array}{c} \text{O} \\    \\ \text{H}_3\text{C}-\text{CH}_2-\text{CH}_2-\text{C}-\text{NH}_2 \end{array}$	87	0.058	$0.03 \pm 0.02(4)$
n-Propyl urea	$\begin{array}{c} \text{O} \\    \\ \text{H}_3\text{C}-\text{CH}_2-\text{CH}_2-\text{NH}-\text{C}-\text{NH}_2 \end{array}$	102	—	$0.21 \pm 0.07(5)$
Isopropyl urea	$\begin{array}{c} \text{O} \\    \\ \text{H}_3\text{C} \quad \text{H}_3\text{C} \quad \text{CH}-\text{NH}-\text{C}-\text{NH}_2 \end{array}$	102	—	$0.24 \pm 0.05(4)$

Table (continued)

Compound <sup>a</sup>	Molecular formula	Mol Wt	Ether: water partition coefficient ( $K_{\text{ether}}$ )	$\sigma^c$
<i>Five-carbon compounds</i>				
Isoamyl alcohol	$\begin{array}{c} \text{H}_3\text{C} \\ \text{H}_3\text{C} \end{array} \text{CH}-\text{CH}_2-\text{CH}_2-\text{OH}$	88	19	$-0.32 \pm 0.08(6)$
2,2-Dimethyl- 1,3-propanediol	$\begin{array}{c} \text{CH}_3 \\ \text{HO}-\text{CH}_2-\text{C}-\text{CH}_2-\text{OH} \\ \text{CH}_3 \end{array}$	104	—	$0.00 \pm 0.00(3)$
1,5-Pentanediol	$\text{HO}-\text{CH}_2-\text{CH}_2-\text{CH}_2-\text{CH}_2-\text{CH}_2-\text{OH}$	104	0.055	$0.05 \pm 0.06(4)$
L-Arabinose		150	—	$0.52 \pm 0.07(12)$
D-Arabinose		150	$3.8 \times 10^{-5}$	$0.98 \pm 0.02(4)$
L-Xylose		150	—	$0.97 \pm 0.02(5)$
Pyridine		79	1.2	$-0.33 \pm 0.14(3)$
n-Valeramide	$\text{H}_3\text{C}-\text{CH}_2-\text{CH}_2-\text{CH}_2-\text{C}(=\text{O})\text{NH}_2$	101	—	$0.02 \pm 0.01(4)$
Isovaleramide	$\begin{array}{c} \text{O} \\ \text{H}_3\text{C} \diagdown \text{CH}-\text{CH}_2-\text{C}=\text{NH}_2 \\ \text{H}_3\text{C} \diagup \end{array}$	101	0.17	$0.02 \pm 0.00(4)$
<i>Six- or more carbon compounds</i>				
1,6-Hexanediol	$\text{HO}-(\text{CH}_2)_6-\text{OH}$	118	0.12	$0.02 \pm 0.02(4)$

Table (continued)

Compound <sup>a</sup>	Molecular formula	Mol Wt	Ether:water partition coefficient <sup>b</sup> ( $K_{\text{ether}}$ )	$\sigma^c$
Pinacol		118	0.43	$-0.02 \pm 0.04(4)$
Dipropylene glycol		134	0.035	$0.04 \pm 0.03(4)$
Triethylene glycol		150	0.0031	$0.51 \pm 0.12(5)$
Inositol		180	—	$1.02 \pm 0.03(5)$
D-Mannitol		182	—	$1.04 \pm 0.05(3)$
D-Glucose		180	$4.5 \times 10^{-6}$	$0.74 \pm 0.06(8)$
L-Glucose		180	$4.5 \times 10^{-6}$	$0.98 \pm 0.01(3)$
Hexamethylene tetramine		140	0.00026	$0.64 \pm 0.10(4)$
1,7-Heptanediol	HO-(CH <sub>2</sub> ) <sub>7</sub> -OH	132	—	$-0.06 \pm 0.04(4)$
Raffinose	C <sub>18</sub> H <sub>32</sub> O <sub>16</sub> ·5H <sub>2</sub> O	595	—	$1.03 \pm 0.08(6)$

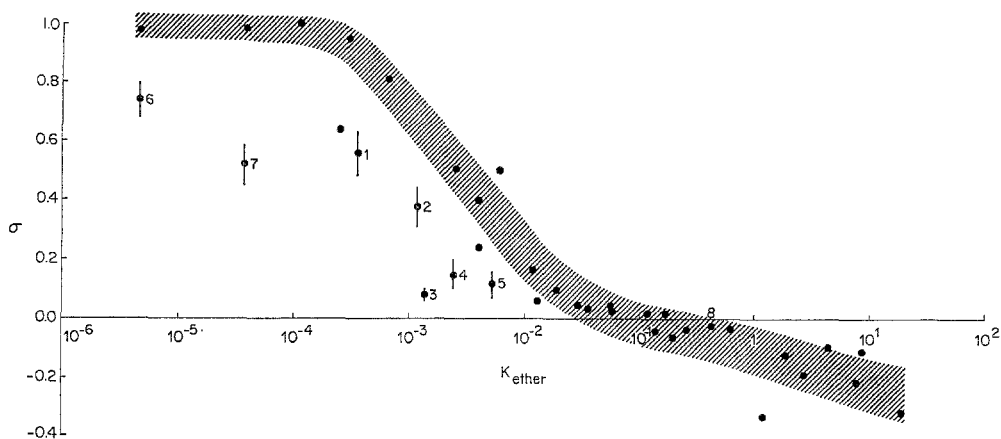


Fig. 3. The relation between  $\sigma$  and the ether:water partition coefficient. The ordinate shows the average  $\sigma$  for nonelectrolytes in the frog choroid plexus; the abscissa shows the ether:water partition coefficient. The numbered points are, 1 urea, 2 methyl urea, 3 formamide, 4 acetamide, 5 ethylene glycol, 6 D-glucose, 7 L-arabinose, and 8 pinacol; the standard deviations are represented by the bars on each point. The shaded band indicates the general pattern of the other points, and, apart from the fact that the width of the band indicates the standard deviation of the results, the band has no theoretical significance. The anomalous position of hexamethylene tetramine ( $\sigma$  0.64,  $K_{\text{ether}}$  0.00026) may be related to the strong basic nature of this compound

molecular weight compounds, the  $\sigma$  for acetamide ( $K_{\text{ether}}=0.0025$ ) was predicted to be about 0.5. Also note that the  $\sigma$ 's for all five compounds are lower than the values predicted from the main pattern. For instance, the actual value measured for acetamide was 0.17. This deviation from the main pattern remains apparent when  $\sigma$  was plotted against  $K_{\text{butanol}}$  or  $K_{\text{olive oil}}$  and for at least two compounds (formamide and acetamide) when the variation in diffusion coefficient was taken into account by plotting  $\sigma$  against  $K_{\text{ether}} \text{ mol wt}^{-1/2}$ ,  $K_{\text{ether}} \text{ mol wt}^{-1}$ , or  $K_{\text{ether}} \text{ mol wt}^{-3}$ . Collander (1954) found empirically that in *Nitella* permeability varied as  $\text{mol wt}^{-1.5}$  for compounds with molecular weights between 70 and 480. The low reflection coefficients obtained for the small polar solutes suggest that they permeate through the membrane at a higher rate than would be predicted from their partition coefficients.

In the gallbladder (Wright & Diamond, 1969*b*) and in giant algae (Collander & Bärlund, 1933; Collander, 1954), it has been observed that, within a homologous series of compounds, permeability increases with increasing chain length from the second or third member onwards, but the first member is generally more permeant than the second. A similar phenomena was observed in the choroid plexus for the amides, dihydroxy alcohols,

monohydroxy alcohols and esters but not for the ureas and thioureas. It can be seen in the Table that  $\sigma$  for the first member of a homologous series was generally no greater and often smaller than the  $\sigma$  for the second; for example, the  $\sigma$  for formamide was  $0.08 \pm 0.02$ (6), whereas the  $\sigma$  for acetamide was  $0.15 \pm 0.05$ (7). This anomalous behavior of these low molecular weight compounds has often been taken as evidence for the mosaic structure of biological membranes (*see* review by Diamond & Wright, 1969*b*).

The reflection coefficients of branched-chain compounds in the rabbit gallbladder were greater than their straight-chain isomers, and the difference was greater than that predicted from their partition coefficients. Comparisons of branched and straight isomers in the choroid plexus can be drawn from the data in the Table, e.g., n-propanol vs. isopropanol; n-propyl urea vs. isopropyl urea; n-valeramide vs. isovaleramide; and 2,2-dimethyl-1,3-propanediol vs. 1,5-propanediol. In contrast with the gallbladder, there is no significant difference between the  $\sigma$ 's for these isomers. The most highly branched compound used in the present study was pinacol

$\left( \begin{array}{c} \text{H}_3\text{C} \\ \diagdown \\ \text{C} \\ \diagup \\ \text{H}_3\text{C} \end{array} \right) - \left( \begin{array}{c} \text{CH}_3 \\ \diagdown \\ \text{C} \\ \diagup \\ \text{CH}_3 \end{array} \right)$  which is point number 8 in Fig. 3. It is apparent from Fig. 3 that the  $\sigma$  for pinacol is close to that expected and is virtually the same as that of the unbranched 1,6-hexanediol.

A further comment to be made about Fig. 3 concerns the optical isomers of glucose and arabinose. D-arabinose and L-glucose  $\sigma$ 's were close to 1, indicating that they were virtually impermeant, as expected from their low partition coefficients.<sup>3</sup> In comparison, the  $\sigma$ 's obtained for L-arabinose and D-glucose were substantially less than 1 (0.52 and 0.74, respectively). The detailed evidence of our following paper (Prather & Wright, 1970) shows that this difference between optical isomers is due to a facilitated diffusion mechanism.

A parameter which has been found useful in the characterization of biological membranes is the number of methylene ( $-\text{CH}_2-$ ) groups that are needed to counterbalance the change in permeability of a molecule brought about by the addition of one hydroxyl group (Diamond & Wright, 1969*a, b*). It can be seen in the Table that the  $\sigma$  for n-propanol ( $-0.12$ ) was not significantly different from the  $\sigma$  for 1,7-heptanediol ( $-0.06$ ); i.e., the increase in  $\sigma$  obtained by the addition of one hydroxyl group to n-propanol

<sup>3</sup> On plotting  $\sigma$  against  $K_{\text{ether}}$ , we assumed that the partition coefficients were identical for the D and L isomers. This assumption appears valid on the grounds that the physical properties (except optical rotation) are identical (Pigman, 1957). The physical properties include melting points which are known to reflect the degree of hydrogen bonding of the solutes.

to form 1,3-propanediol was offset by the addition of four  $-\text{CH}_2-$  groups. Similarly, the  $\sigma$  for ethylene glycol monomethyl ether ( $-0.06$ ) was close to the  $\sigma$  for triethylene glycol ( $0.04$ ), suggesting that slightly more than two  $-\text{CH}_2-$  groups offset the addition of one hydroxyl group to this molecule. Therefore, the decrease in permeability produced by one hydroxyl group is counterbalanced by two to four methylene groups.

## Discussion

### *General Properties of the Choroid Plexus*

The p.d. across the *in vitro* choroid plexus was normally close to zero; this is similar to that observed in the gallbladder (Diamond, 1962; Diamond & Harrison, 1966) and in the small intestine in the absence of actively transported sugars (Barry, Dikstein, Matthews, Smyth & Wright, 1964). The conductance of the choroid plexus was about one-third of that in the gallbladder (Wright & Diamond, 1968), which implies that the choroid plexus is less permeable to ions than is the gallbladder. The polarity of the streaming potential, hypertonic solution positive, shows that cations are more permeant than anions at normal pH. The magnitude of the streaming potentials was lower in the choroid plexus than in the gallbladder and intestine, but it is not known whether this is due to a lower  $L_p$  or to a higher ratio of anion-to-cation permeability. The thick unstirred layers, ca.  $300 \mu$ , are probably due to the villi which project into the ventricular solution.

As indicated in footnote 1, these apparent streaming potentials probably have three components: the true electrokinetic streaming potential, a profile asymmetry potential and a boundary diffusion potential. The boundary diffusion potential, or more correctly the membrane diffusion potential, is caused by sweeping-away effects which produce a local salt concentration gradient across the membrane. Vargas (1968) has calculated that some 25 to 50% of the total potential observed in the squid giant axon was a true streaming potential. The importance of the unstirred layer phenomena has been demonstrated in studies of electroosmosis in artificial membranes (Stewart & Graydon, 1957), giant algal cells (Barry & Hope, 1969*a, b*), and in rabbit gallbladder (Wedner & Diamond, 1969). At present we have no estimate of the relative importance of the three components in the choroid plexus.

### *The Permeability of the Choroid Plexus to Nonelectrolytes*

In this study, the parameter used to measure permeability was the reflection coefficient. Reflection coefficients were determined by a rapid



osmotic procedure introduced first for the small intestine and later used extensively for the gallbladder. Collander (1954) has previously established that osmotic procedures yield the same nonelectrolyte permeability sequences as direct chemical analysis.

The present method is based on the fact that osmotic flow across a charged membrane produces apparent streaming potentials. Although we have not yet been able to verify experimentally that streaming potentials are directly proportional to the rate of osmotic flow in the choroid plexus (because of experimental difficulties), the procedure appears to be valid for three compelling reasons: (1) the streaming potentials in the choroid plexus are very similar to those in other biological membranes where the proportionality between the p.d. and the osmotic flow has already been established (*see Results*); (2) the results obtained by this method in the choroid plexus are very similar to those obtained for the distribution of solutes between blood and brain *in vivo* (*see below*); and (3) we confirmed the selectivity of a few solutes by direct flux measurements (Prather & Wright, 1970).

The validity of the electrical procedure for determining nonelectrolyte permeation through the choroid plexus rests on the assumption that the solutes do not give p.d. except by osmotic flow. Possible sources of uncertainty are that solutes modify active transport potentials or existing transepithelial diffusion potentials, set up transport potentials, and modify the permeability characteristics of the epithelium. These uncertainties are eliminated by the following considerations. (1) In the absence of osmotic gradients, the p.d. across the epithelium is close to zero (*see Results*). (2) The active transport of ions does not generate transport potentials across the choroid plexus (Wright, *unpublished*). (3) Transepithelial diffusion potentials cannot arise during these experiments because the ionic composition of the saline on each side of the preparation is identical. (4) There is close agreement between the  $\sigma$ 's obtained from each side of the plexus (e.g., Table 2 of Prather & Wright, 1970). (5) There is no significant difference between the sucrose streaming potentials measured immediately before and after each test solute. (6) The solutes do not produce anomalous streaming potential transients. (7) The  $\sigma$ 's are independent of concentration (except for some sugars; *see Fig. 1* of Prather & Wright, 1970). (8) Solutes which may be expected to produce transport potentials, e.g., sugars, fail to change the p.d. when added to both the ventricular and serosal solutions to give concentrations within the physiological range. (9) The patterns of nonelectrolyte selectivity obtained in the choroid plexus agree closely with those in the classical literature.

The reference nonelectrolyte used to determine reflection coefficients was sucrose (12 carbons). The epithelium of the choroid plexus was judged to be impermeable to sucrose (i.e.,  $L_p \gg \omega \bar{V}_c$ ) since the reflection coefficients for 15 fully hydroxylated (4 to 18 carbon) compounds were indistinguishable from 1.0. Owing to the unstirred-layer effects discussed earlier, the nonelectrolyte  $\sigma$ 's obtained in this study are not "true"  $\sigma$ 's but are relative values. Consequently, we have limited our discussion of the results to those conclusions that can be drawn without the knowledge of unstirred-layer corrections. Our confidence in this approach has been confirmed recently on finding that the electrical procedure for determining  $\sigma$ 's and radioactive tracer permeability measurements yields the same selectivity sequences in the gallbladder (Smulders & Wright, *unpublished*). Finally, although ultrastructure studies have shown that it is the epithelial layer which provides the barrier to the movement of solutes across the choroid plexus (Brightman & Reese, 1969), we are unable to specify at present the relative contributions of each epithelial cell face.

The present investigation shows that the permeability characteristics of the choroid plexus are very similar to those of the giant algae (Collander & Bärilund, 1933; Collander, 1954) and of the rabbit gallbladder (Wright & Diamond, 1969*b*). In these membranes, nonelectrolyte permeability generally increases with increasing lipid:water partition coefficients. Therefore, the same solute:water and solute:lipid intermolecular forces that control the distribution of solutes between a bulk lipid solvent and water also control the rate of permeation of most solutes through cell membranes. Thermodynamic analysis (Diamond & Wright, 1969*b*) has shown that nonelectrolyte selectivity patterns observed in such diverse systems as the bulk lipid solvents and biological membranes were largely controlled by differences in solute:water intermolecular attractive forces; the stronger these forces, the lower the partition coefficient and the lower the permeability. The quantitative differences between selectivity patterns, however, are largely due to differences in solute:lipid intermolecular forces in different membranes; the weaker these forces, the greater the spread of the selectivity pattern (Diamond & Wright, 1969*b*). The nature of these forces was analyzed by Collander (1949), Stein (1967) and Diamond and Wright (1969*a, b*). The chief solute:water intermolecular forces were identified as hydrogen bonds and entropy effects in hydrocarbon:water interactions. Although the weak van der Waal's intermolecular forces are probably the principal solute:lipid intermolecular forces, it was recognized that the number of hydrogen bonding sites in the membrane lipids was important. Undoubtedly it is the balance between solute:water and solute:lipid intermolecular forces which governs the permeability of the choroid plexus to most nonelectrolytes.

The general form of Fig. 3 is very similar to the relationship observed between  $\sigma$  and  $K_{\text{ether}}$  in the rabbit gallbladder. On close examination, however, there are three differences of detail. (1) In the choroid plexus, the  $\sigma/K_{\text{ether}}$  curve is appreciably to the left of the gallbladder curve; i.e.,  $\sigma$ 's for permeant solutes are considerably smaller in the choroid plexus than in the gallbladder. For example, in the choroid plexus, the  $\sigma$  was 0.42 for diethylene glycol and 0.05 for 2,3-butanediol, compared with 0.92 and 0.74, respectively, in the gallbladder. (2) The middle portion of the choroid plexus curve is less steep. In the choroid plexus,  $\sigma$  is reduced from 0.9 to 0.1 by a 40-fold increase in  $K_{\text{ether}}$ , whereas in the gallbladder the same reduction in  $\sigma$  is brought about by a 20-fold increase in  $K_{\text{ether}}$ . (3) Negative  $\sigma$ 's were not obtained in the gallbladder.

The reason for these differences between the choroid plexus and the gallbladder cannot be stated unequivocally at present because the reflection

coefficient of a solute is set by three parameters: the  $L_p$ , the permeability coefficient  $\omega$ , and the magnitude of the unstirred layer (see 3rd section of Results). It is known from the half times of the streaming potentials that the thicknesses of the unstirred layers are greater in the choroid plexus than in the gallbladder, but in the absence of  $L_p$  and  $\omega$ 's it is difficult to evaluate which of these parameters accounts for the differences between the two membranes. However, some insight into this problem can be obtained by comparing the number of methylene ( $-\text{CH}_2-$ ) groups that it requires to counterbalance the change in  $\sigma$  produced by one hydroxyl group. In the choroid plexus, it requires two to four methylene groups to balance one hydroxyl group, whereas in the gallbladder it requires about six methylene groups (Diamond & Wright, 1969*a*). This suggests that the membrane lipids of the choroid plexus contain a higher ratio of hydrogen bonding sites to methylene groups than do the lipids of the gallbladder; i. e., stronger solute:lipid intermolecular forces exist in the choroid plexus. The higher this ratio, the lower the magnitude of selectivity (see Diamond & Wright, 1969*b*, for further discussion). Therefore, at least some of the differences between  $\sigma$ 's in the gallbladder and choroid plexus could be due to differences in lipid structure.

Additional evidence pointing to differences in lipid structure is that there is no apparent difference between the  $\sigma$ 's for straight- and branched-chain analogues. This is in contrast to the gallbladder where the  $\sigma$ 's for branched-chain compounds were greater than predicted from their partition coefficients in bulk lipids (Wright & Diamond, 1969*b*). Most cell membranes discriminate against branched compounds and this has been attributed to the highly ordered configuration of the membrane lipids (see Diamond & Wright, 1969*b*). On the basis of this interpretation, the membrane lipids of the choroid plexus appear to be less rigidly orientated. A similar conclusion would apply to the mesophyll cells of the plant *Vallisneria* which plasmolyze at much the same rate in either erythritol or pentaerythritol solutions (Collander, 1959).

Negative reflection coefficients were not obtained in the gallbladder, but values as low as  $-0.3$  were obtained in the choroid plexus. Gutknecht (1968) also obtained negative reflection coefficients in the marine alga *Valonia*. However, at the higher ranges of the partition coefficients,  $\sigma$ 's level off in both the choroid plexus and the gallbladder, indicating that at high rates of solute permeation solute diffusion through the unstirred layers becomes rate limiting. The simplest consistent interpretation of both the negative  $\sigma$ 's and the shift to the left of the  $\sigma/K_{\text{ether}}$  curve in the choroid plexus is that the ratio of nonelectrolyte permeability coefficients to the

water permeability coefficient is higher in the choroid plexus than in the gallbladder.

The behavior of the small polar solutes is anomalous in that they tend to permeate through the choroid plexus at a greater rate than would be predicted from their partition coefficients. In other membranes, this has been used to support the notion that small solutes permeate via polar regions in the membrane (Wright & Diamond, 1969*b*). Because of the scatter in the results, the small number of high molecular weight compounds available with partition coefficients in the appropriate range and the fact that the membrane lipids constitute a major permeation pathway for these solutes, the choroid plexus results taken alone would not suffice to prove the existence of a separate polar pathway, although the analogy with the results from the gallbladder and *Nitella* suggest that this is the correct interpretation. However, the present results do confirm the previous contention that it is unjustifiable to assume without proof that the small polar solutes such as urea permeate biological membranes exclusively through pores (Wright & Diamond, 1969*b*), since Fig. 3 shows that the  $\sigma$ 's for urea, methyl urea, formamide, acetamide and ethylene glycol in the choroid plexus would be well below 1 owing to permeation through lipid even in the absence of a polar route. Consequently, it is essential to establish that the probing molecules used to determine "equivalent pore radii" do not permeate via the membrane lipids. In the choroid plexus, the polar route must only be of significance for one- and two-carbon compounds since the  $\sigma$ 's for three-, four- and higher carbon compounds are close to the main pattern; e. g., erythritol  $\sigma = 1.0$ .

A special permeation mechanism is indicated for the monosaccharides since D-glucose and L-arabinose  $\sigma$ 's are lower than the  $\sigma$ 's for their optical isomers and are lower than predicted from their partition coefficients. The mechanism of sugar transport is explored further in the accompanying paper (Prather & Wright, 1970) where it is shown that the process is facilitated diffusion. This is in agreement with the previous findings of Bradbury and Davson (1964) and Fishman (1964) on the distribution of sugar between the blood and CSF.

#### *Comparison with In Vivo Studies*

In general, there is good agreement between the results presented here and the previous *in vivo* studies of the distribution of material between the blood and CSF. For example, the importance of "lipid solubility" in governing the rate of penetration of nonelectrolytes (Davson, 1955) and of drugs (Brodie, Kurz & Schanker, 1960) into the CSF has been well estab-

lished. A quantitative comparison of the *in vitro* and the *in vivo* data is excluded at the present time owing to the fact that the passage of material into the CSF from blood involves both the choroid plexuses and the "blood brain barrier". The permeability characteristics of the "blood brain barrier" (Crone, 1965*a*) are at least qualitatively very similar to those of the choroid plexus. The equivalent pore radius of the "blood brain barrier" has been estimated to be 7 to 9 Å by Fenstermacher and Johnson (1966) on the basis of five reflection coefficient measurements. This is certainly an overestimate of the pore size, because at least one of their probing molecules, glucose, does not permeate the barrier exclusively through pores. Crone (1965*b*) has provided evidence for the facilitated transport of glucose across the "blood brain barrier".

It can be concluded that the epithelium of the frog choroid plexus constitutes a barrier to the distribution of nonelectrolytes between blood and the CSF. The permeability characteristics of the barrier are qualitatively similar to those exhibited by other cell membranes. Consequently, it is to be expected that the frog choroidal epithelium takes an active role in the regulation of the composition of the CSF.

We take pleasure in acknowledging Drs. Jared M. Diamond and Peter H. Barry for their valuable discussion throughout this study and for their critical reading of the manuscript, and Drs. I. Cameron and R. S. Eisenberg for their critical reading of the manuscript.

This study was supported by grants from the Los Angeles County Heart Association and a program project from the U.S. Public Health Service (HE 11351). One of us (J.W.P.) was a Postdoctoral Fellow under U.S. Public Health Service training grant 5T01 HE 5696.

## References

- Barry, P. H., Hope, A. B. 1969*a*. Electroosmosis in membranes: Effects of unstirred layers and transport numbers. I. Theory. *Biophys. J.* **9**:700.  
— — 1969*b*. Electroosmosis in membranes: Effects of unstirred layers and transport numbers. II. Experimental. *Biophys. J.* **9**:729.  
Barry, R. J. C., Dikstein, S., Matthews, J., Smyth, D. H., Wright, E. M. 1964. Electrical potentials associated with intestinal sugar transfer. *J. Physiol.* **171**:316.  
Bradbury, M. W. B., Davson, H. 1964. The transport of urea, creatinine and certain monosaccharides between blood and fluid perfusing the cerebral ventricular system of rabbits. *J. Physiol.* **170**:195.  
Brightman, M. W., Reese, T. S. 1969. Junctions between intimately opposed cell membranes in the vertebrate brain. *J. Cell Biol.* **40**:648.  
Brodie, B. B., Kurz, H., Schanker, L. S. 1960. The importance of dissociation constant and lipid-solubility in influencing the passage of drugs into the cerebrospinal fluid. *J. Pharmacol.* **130**:20.  
Carpenter, S. J. 1966. An electronmicroscopic study of the choroid plexus of necturus maculosus. *J. Comp. Neurol.* **127**:413.

- Collander, R. 1947. On "lipid solubility". *Acta Physiol. Scand.* **13**:363.
- 1949. Die Verteilung organischer Verbindungen zwischen Äther und Wasser. *Acta Chem. Scand.* **3**:717.
- 1954. The permeability of *Nitella* cells to non-electrolytes. *Physiol. Pl.* **7**:420.
- 1959. Das Permeationsvermögen des Pentaerythrits verglichen mit dem des Erythrits. *Physiol. Pl.* **12**:139.
- Bärlund, H. 1933. Permeabilitätsstudien an *Chara Ceratophylla*. II. Die Permeabilität für Nichtelektrolyte. *Acta Bot. Fenn.* **11**:1.
- Crone, C. 1965*a*. The permeability of brain capillaries to non-electrolytes. *Acta Physiol. Scand.* **58**:292.
- 1965*b*. Facilitated transfer of glucose from blood to brain tissue. *J. Physiol.* **181**:103.
- Dainty, J. 1963. Water relations of plant cells. *Advanc. Bot. Res.* **1**:279.
- Davson, H. 1955. A comparative study of the aqueous humour and cerebrospinal fluid in the rabbit. *J. Physiol.* **129**:111.
- 1967. *Physiology of the Cerebrospinal Fluid*. Churchill, London.
- Diamond, J. M. 1962. The mechanism of water transport by the gallbladder. *J. Physiol.* **161**:503.
- 1966. A rapid method for determining voltage-concentration relations across membranes. *J. Physiol.* **183**:83.
- Harrison, S. C. 1966. The effect of membrane fixed charges on diffusion potentials and streaming potentials. *J. Physiol.* **183**:37.
- Wright, E. M. 1969*a*. Molecular forces governing non-electrolyte permeation through cell membranes. *Proc. Roy. Soc. (London) B* **172**:273.
- — 1969*b*. Biological membranes: The physical basis of ion and non-electrolyte selectivity. *Ann. Rev. Physiol.* **31**:581.
- Dietschy, J. M. 1964. Water and solute movement across the wall of the everted rabbit gall bladder. *Gastroenterology* **47**:395.
- Fenstermacher, J. D., Johnson, J. A. 1966. Filtration and reflection coefficients of the rabbit blood-brain barrier. *Amer. J. Physiol.* **211**:341.
- Fishman, R. A. 1964. Carrier transport of glucose between blood and cerebrospinal fluid. *Amer. J. Physiol.* **206**:836.
- Gutknecht, J. 1968. Permeability of *Valonia* to water and solutes: Apparent absence of aqueous membrane pores. *Biochim. Biophys. Acta* **163**:20.
- Katchalsky, A., Kedem, O. 1962. Thermodynamics of flow processes in biological systems. *Biophys. J.* **2**(pt 2):53.
- Lasansky, A., de Fisch, F. W. 1966. Potential, current, and ionic fluxes across the isolated retinal pigment epithelium and choroid. *J. Gen. Physiol.* **49**:913.
- Patlak, C. S., Adamson, R. H., Oppelt, W. W., Rall, D. P. 1966. Potential difference of the ventricular fluid in vivo and in vitro in the dogfish. *Life Sci.* **5**:2011.
- Pidot, A. L., Diamond, J. M. 1964. Streaming potentials in a biological membrane. *Nature* **201**:701.
- Pigman, W. W. (Ed.) 1957. *The Carbohydrates: Chemistry, Biochemistry, Physiology*. Academic Press, New York.
- Prather, J. W., Wright, E. M. 1970. Molecular and kinetic parameters of sugar transport across the frog choroid plexus. *J. Membrane Biol.* **2**:150.
- Schmid, G., Schwarz, H. 1962. Zur Elektrochemie feinporiger Kappillarsysteme. V. Strömungspotentiale; Donnan-Behinderung des Electrolytdurchgangs bei Strömungen. *Z. Electrochem.* **56**:35.
- Sherry, H. S. 1969. The ion exchange properties of the zeolites. *In: Ion Exchange*, vol. 2. J. A. Marinsky, editor. Marcel Dekker, New York.
- Smyth, D. H., Wright, E. M. 1966. Streaming potentials in the rat small intestine. *J. Physiol.* **182**:591.

- Staverman, A. J. 1951. The theory of measurement of osmotic pressure. *Rec. Trav. Chim. Pays-Bas* **70**:344.
- Stein, W. D. 1967. Movement of molecules across cell membranes. *In: Theoretical and Experimental Biology*, vol. 6. Academic Press, New York.
- Stewart, R. J., Graydon, W. F. 1957. Ion-exchange membranes. III. Water transfer. *J. Phys. Chem.* **61**:164.
- Wedner, H. J., Diamond, J. M. 1969. Contributions of unstirred-layer effects to apparent electrokinetic phenomena in the gall bladder. *J. Membrane Biol.* **1**:92.
- Wright, E. M., Diamond, J. M. 1968. Effects of pH and polyvalent cations on the selective permeability of gall bladder epithelium to monovalent ions. *Biochim. Biophys. Acta* **163**:57.
- — 1969a. An electrical method of measuring non-electrolyte permeability. *Proc. Roy. Soc. (London) B* **172**:203.
- — 1969b. Patterns of non-electrolyte permeability. *Proc. Roy. Soc. (London) B* **172**:227.
- Vargas, F. F. 1968. Water flux and electrokinetic phenomena in the squid axon. *J. Gen. Physiol.* **51**:123s.